BOLETIN DE LA SOCIEDAD ESPAÑOLA DE
Cerámica y Vidrio
A R T I C U L O

Processing of Samarium Doped Ceria for IT-SOFC. Grain Boundary Effect on the Electrical Conductivity

C. SÁNCHEZ-BAUTISTA*, A. J. DOS SANTOS-GARCÍA, J. PEÑA-MARTÍNEZ, J. CANALES-VÁZQUEZ*

Instituto de Investigación en Energías Renovables, Universidad de Castilla La Mancha, Parque Científico y Tecnológico de Albacete, Paseo de la Investigación 1, 02006 Albacete.

Nanometric powders of ceria doped with 10, 15 and 20% at. of samarium were prepared by a sol-gel method. The powders were compacted in cylindrical pellets and sintered at different temperatures in order to obtain grain sizes ranging from 1 to 10 microns. The electrical conductivity was measured in air by electrochemical impedance spectroscopy in the 1166 - 473 K temperature range. The bulk and grain boundary contributions to the overall conductivity were estimated by equivalent circuit analysis and the application of the brick layer model. While bulk conductivity values were markedly independent of the grain size, a relevant decrease in the grain boundary specific conductivity was observed for the finer grain samples in the lower dopant grade. For increased samarium content, this decrease in specific grain boundary conductivity with grain size becomes less relevant.

Keywords: doped ceria, electrolyte, ionic conductivity, brick layer model, IT-SOFC

Procesado de Óxido de Cerio dopado con samario para su aplicación en IT-SOFC. Efecto del límite de grano en la Conductividad Eléctrica

En el presente trabajo de investigación se han obtenido satisfactoriamente, muestras policristalinas de ceria dopada con 10, 15 y 20% at. de samario sintetizadas por el método sol-gel. Cada una de las muestras, previamente calcinadas, fueron compactadas y posteriormente sinterizadas a diferentes temperaturas con el fin de obtener distintos tamaños de grano que, como posteriormente se ha observado, oscilan en un rango de 1 a 10 micrómetros. La conductividad eléctrica de las pastillas densas se midió en atmósfera de aire, mediante la técnica de espectroscopía de impedancia electroquímica en el rango de temperatura de 1166-473 K. Las contribuciones del interior y del límite de grano a la conductividad total se estimaron mediante un análisis/ajuste por circuitos equivalentes aplicando el "*brick layer model*". Es interesante señalar que los valores de conductividad del interior del grano son independientes del tamaño del mismo; por otro lado, en las muestras ligeramente dopadas con samario puede observarse una notoria disminución del valor de conductividad específica de límite de grano. No obstante, para mayores contenidos en samario, esta disminución es menos notoria.

Palabras clave: ceria dopada, electrolito, conductividad iónica, brick layer model, IT-SOFC

1. INTRODUCTION

Rare-earth doped cerias have received a great deal of attention and have become a major topic of research for many groups over the world. One of the main reasons for this interest is the elevated ionic conductivity at low temperatures (below 773 K), which turn them into potential electrolytes for intermediate temperature solid oxide fuel cells (IT-SOFC).

Nevertheless there are also some drawbacks associated to the use of ceria-based materials, such as the readiness to reduction of Ce^{4+} to Ce^{3+} with low oxygen partial pressure and/or elevated temperatures and the subsequent appearance of electronic conductivity. Thus, 773 K is the typical design operating temperature, and as several authors have alleged, the reasons to consider ceria based materials as electrolytes for SOFC beyond 873 K are weak (1).

Typical sintering temperatures for ceria-based electrolytes processed by the ceramic method are in the range of 1773-1873 K. However, the development of wet techniques for the production of nanometric precursors has permitted to lower these temperatures below 1673 K. The combined use of high uniaxial or isostatic pressure and nanometric precursor powders, reduces the sintering temperature down to 1273 K (2,3), leading to samples with nanometric grain size. However, these processing parameters may complicate the practical implementation for SOFC manufacturing, since these elevated pressures are normally attainable for specimens with reduced area.

A further technological barrier to the practical implementation of nanometric grain sized electrolytes is the high temperature generally required to attach the electrodes (typically 1473 K and higher), which may induce grain coarsening at the micrometric scale. In this scenario, the optimisation of the electrochemical properties of doped ceria electrolytes in the micrometric grain size range is still of maximum interest.

The overall electrical response of a polycrystalline electrolyte is a function of bulk and grain boundary resistivity. It has been commonly observed (4,5) that the specific grain boundary conductivity is several orders of magnitude lower than the bulk contribution, and attending to the typical higher activation energy of the grain boundary conduction process, it may become extremely significant in the low temperature operating regime.

During the last decades, the blocking effect of the grain boundary area has been attributed to the presence of a siliceous phase; although this is only relevant in materials of average to low purity, an important blocking effect has also been observed in high purity materials, where the continuity of the siliceous phase is highly unlikely. In this second case, the formation of space charge layers which compensate the positive net charge originated by the accumulation of oxygen vacancies in the grain boundary core is responsible for the significant decrease in the electrical conductivity. Moreover, it has been pointed out that the grain boundary specific conductivity increases when the grain size is reduced (6, 7). Zhou *et al.* (8) also observed a similar behaviour for $Ce_{0.9}Gd_{0.1}O_{1.95}$, however, the increase in grain boundary volume resulted in higher overall resistance. Following the same trend, Mori *et al.* have shown in several works (2,9,10) how the overall electrical conductivity for ceria doped with different rare earths exhibits a V-shape curve as a function of grain size, and the minimum of conductivity varies with grain size and the rare earth employed for doping.

These results highlight the need for more experimental research on this topic since the variation of grain boundary specific conductivity seems to be not only dependent on grain size but also on dopant grade and on the rare earth selected. Therefore, it is of high interest to determine if, under technologically conventional processing parameters, there exists a range of compositions where finer grain sized electrolyte may offer better overall responses.

2. EXPERIMENTAL

2.1. Synthesis

Powders of Sm-doped ceria with samarium contents of 10, 15 and 20% at. were prepared by a modified sol-gel method. $Ce(NO_3)_3{\cdot}6H_2O$ (Sigma Aldrich, ≥99%) and $Sm(NO_3)_3{\cdot}6H_2O$ (Alfa Aesar, ≥99.5%) where weighed in the appropriate ratio to obtain $Ce_{0.9}Sm_{0.1}O_{1.95}$ (SDC10), $Ce_{0.85}Sm_{0.15}O_{1.925}$ (SDC15) and $Ce_{0.8}Sm_{0.2}O_{1.90}$ (SDC20), and mixed with distilled water. Citric acid (Sigma Aldrich, reagent grade) and ethylene glycol (Sigma Aldrich, ≥99%) were added as chelating and gel-former agents respectively. Under mild stirring, the solution was slowly heated up to 328 K in a hot plate to form a viscous transparent gel. When the gel was formed, the temperature was elevated to 673 K and the subsequent evaporation, partial decomposition and auto ignition of the hard gel resulted in the formation of a yellowish powder precursor. The precursor was fired in a range of temperatures (873-973 K) and periods of time (3-10 hours) in order to eliminate the remaining organics. Afterwards, overnight ball milling with zircona balls and containers at 100 rpm in high purity acetone medium was performed with the aim of reducing the extent of hard agglomerates.

The resulting powders were dried and compacted under 250 MPa to form green pellets of 10 mm of diameter and

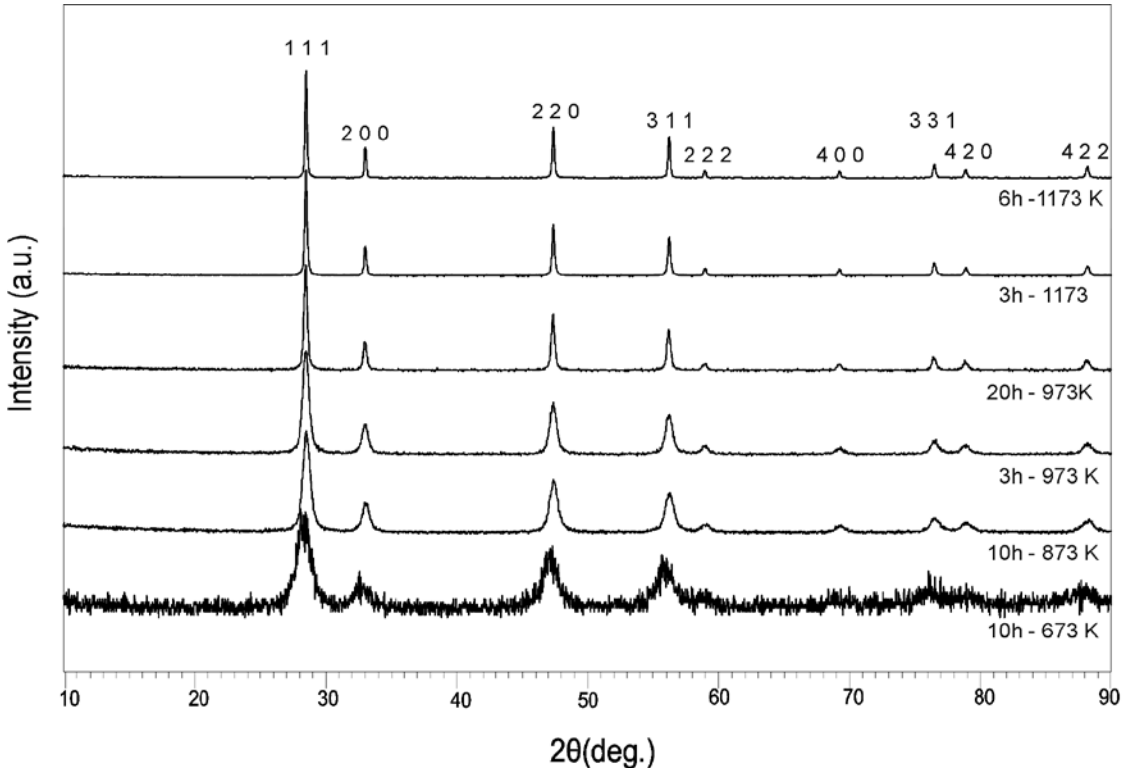

Figure 1. XRD patterns of several SDC10 precursors

approximately 1 mm of thickness. The pellets were sintered at 1623 K, 1673 K and 1773 K for 24 hours. This extended sintering time aims to obtain a fully dense and stable microstructure.

2.2. Characterisation

All the precursors were characterised by X-ray powder diffraction (XRD) performed in a PANalytical diffractometer equipped with a X'Celerator detector with monochromatic $CuK_{\alpha 1}$ radiation (λ = 1.54056 Å). XRD patterns were performed in the 5º to 120º 2θ range with a scan step size of 0.017. Rietveld refinements of the data were performed using the Fullprof Suite program. The backgrounds were fitted using four background parameters and peak shapes were modeled by a Thompson Cox Hasting function. The apparent particle sizes were determined from the 422 reflection using the Scherrer formula: $D_{app}=0.93\lambda/\beta\cos\theta$ where λ is the $CuK_{\alpha 1}$ wavelength and $\beta=(\beta_m-\beta_s)$ is the corrected half-width of the β_m-422 reflection. β_s is the half-width of the 422 reflection of the non-doped CeO_2 sample, synthesised under the same conditions.

In all cases the density was >95% and for higher sintering temperatures around 99%. The average grain size was calculated by means of the linear intercept method, with at least 100 interceptions and considering a correction factor of 1.56 (9) to attain true grain size.

Pt electrodes were deposited on both sides of the pellets and then fired at 1173 K for 30 minutes. AC Electrochemical Impedance Spectroscopy (EIS) measurements were performed using a Solartron 1470E CellTest System in the 1166 K to 473 K temperature range, with frequencies ranging from 1 to 10^6 Hz applying a 25 mV signal. At low temperatures (typically below 650 K), different contributions to the overall impedance were separated and ascribed to bulk, grain boundary and electrode responses by equivalent circuit analysis (Zplot software, Scribner Associates (11)).

3. RESULTS AND DISCUSSION

3.1. Phase structure and microstructural evolution

The experimental results show a marked influence of the calcination process of the sol-gel product on the final precursor particle size. Obviously, the particle size became larger with increasing the calcination temperature, e.g. at the lowest temperatures tested, i.e. 673 K, the particle size did not exceeded 15 nm, while higher temperatures (1173 K) led to larger sizes of around 70 nm for SDC10 precursors. More detailed analysis on variation of particle size with calcining temperature will be discussed elsewhere (12). Figure 1 shows several XRD patterns corresponding to different tested temperature-time profiles for SDC10 precursors. Even at low firing temperatures, the main reflections of a single phase fluorite-type structure can be unambiguously identified. The lattice parameters were calculated after Rietveld refinement and ranged between 5.4266(1) Å for SDC10, 5.4299(7) Å for SDC15 and 5.4369(1) Å for SDC20, which is in agreement with the results published in the literature (13).

In all cases, under a compacting pressure of 250 MPa it has been possible to reach densities over 95% with the largest particle size by sintering at 1773 K, i.e. sol-gel product calcined for 6 hours at 1173 K. However, when the sintering temperature is lowered, finer precursors are required to produce nearly fully dense samples. For instance, all the samples sintered at 1623 K were obtained from powders with particle size lower than 30 nm. However it should be noted that the doping level plays an important role and larger amounts of the substituting rare-earth results in samples exhibiting more difficulties to achieve full density upon sintering (14). Indeed the density of the SDC20 samples sintered below 1673 K were around 90% and, considering that nearly full density is recommended for an appropriate use of brick layer model (15), were discarded for this study.

TABLE I. SELECTED DATA OF SDC10, SDC15 AND SDC20 CERAMICS.

Sample	$T_{sintering}$ (K)	Density (%)	Average grain size (μm)	Grain Boundary thickness δ(nm)	α_{gb}
SDC10	1773	99	7	4.7±0.5	0.93
	1673	95	3.4	4.7±0.1	0.84
	1623	94	1.8	3.6±0.2	0.85
SDC15	1773	99	9	4.5±0.7	0.69
	1673	99	3	3.9±0.4	0.85
	1623	95	1.9	2.7±0.2	0.88
SDC20	1773	98	8.4	3.3±0.2	0.73
	1673	94	5	4.1±0.2	0.74

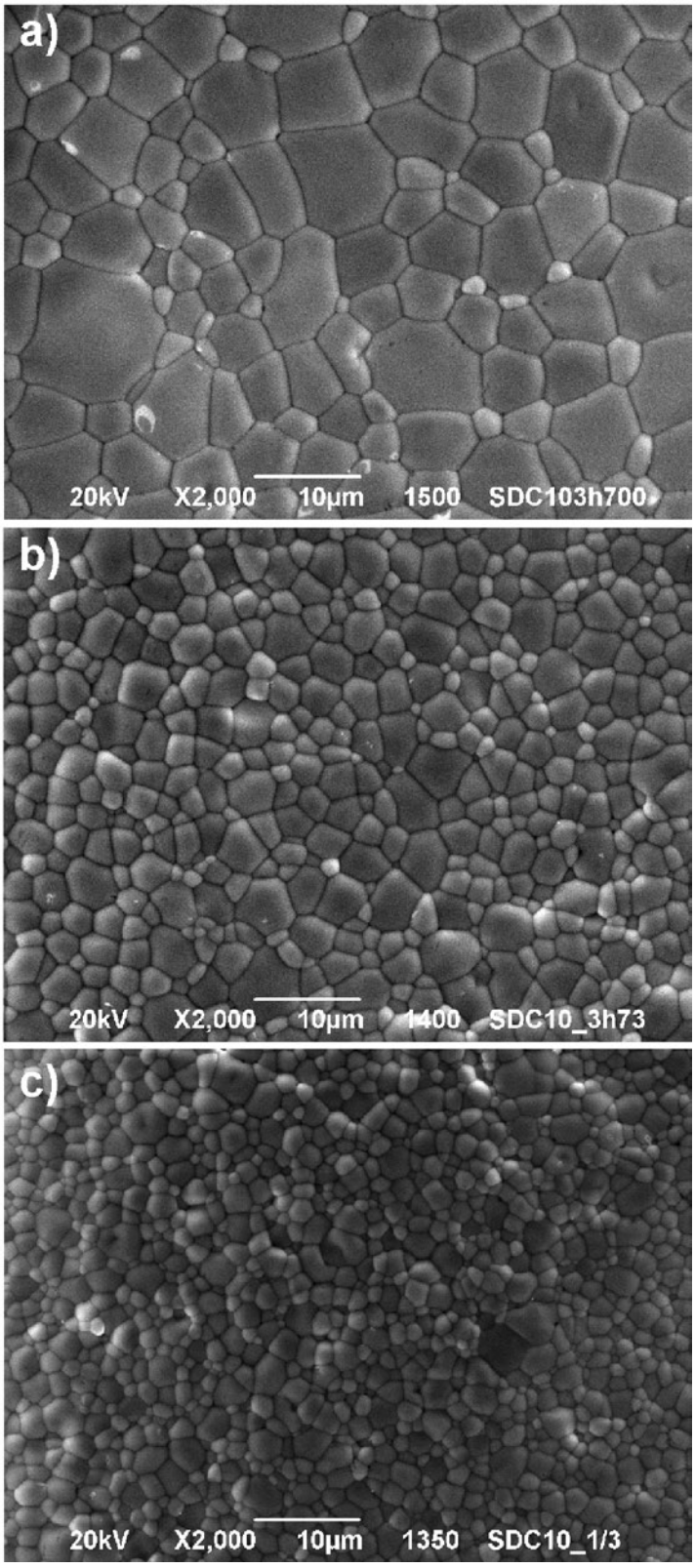

Figure 2. Evolution of the microstructure of SDC10 pellets with sintering temperature a) 1773 K b) 1673 K and c) 1623 K

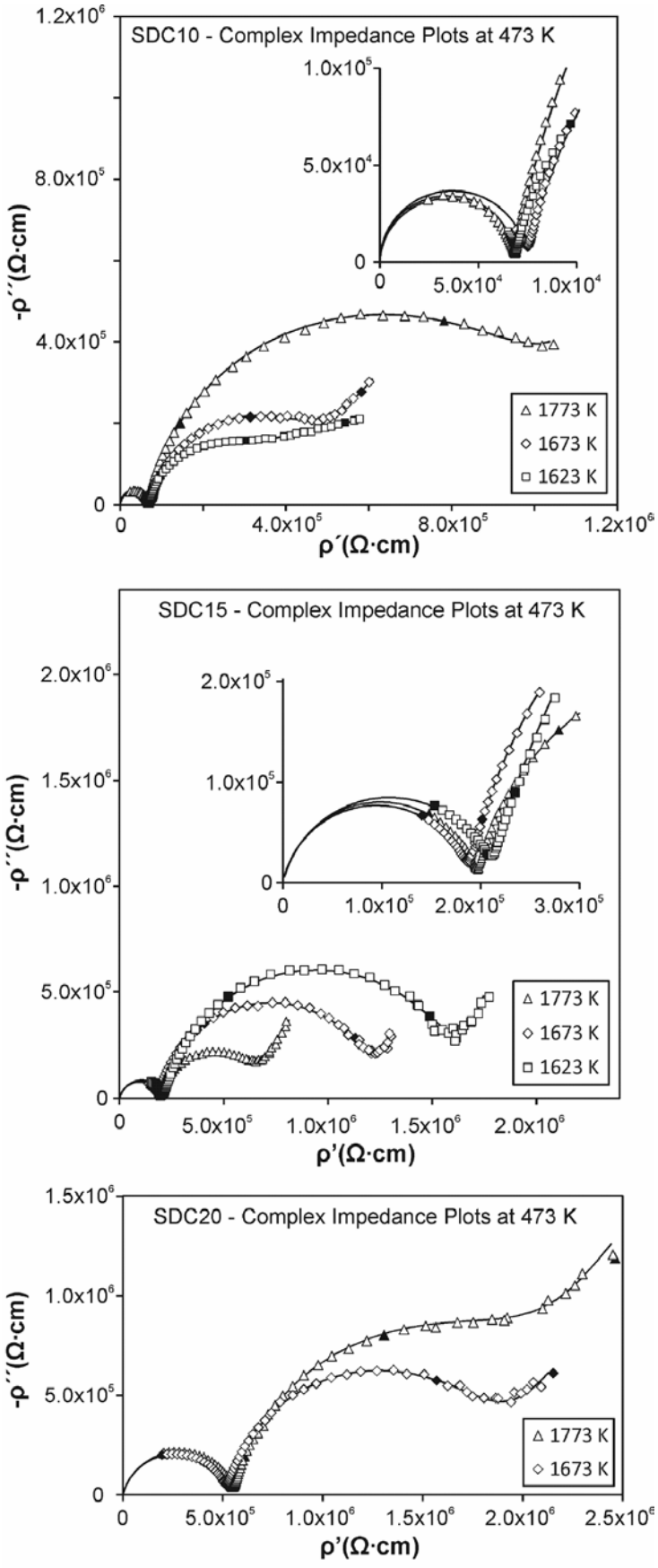

Figure 3. Complex Impedance plots of SDC10 (up), SDC15 (middle) and SDC20 (bottom) samples measured at 473 K. Continuous lines represent the simulated data resulting from the equivalent circuit analysis while discrete points are the result from impedance measurements

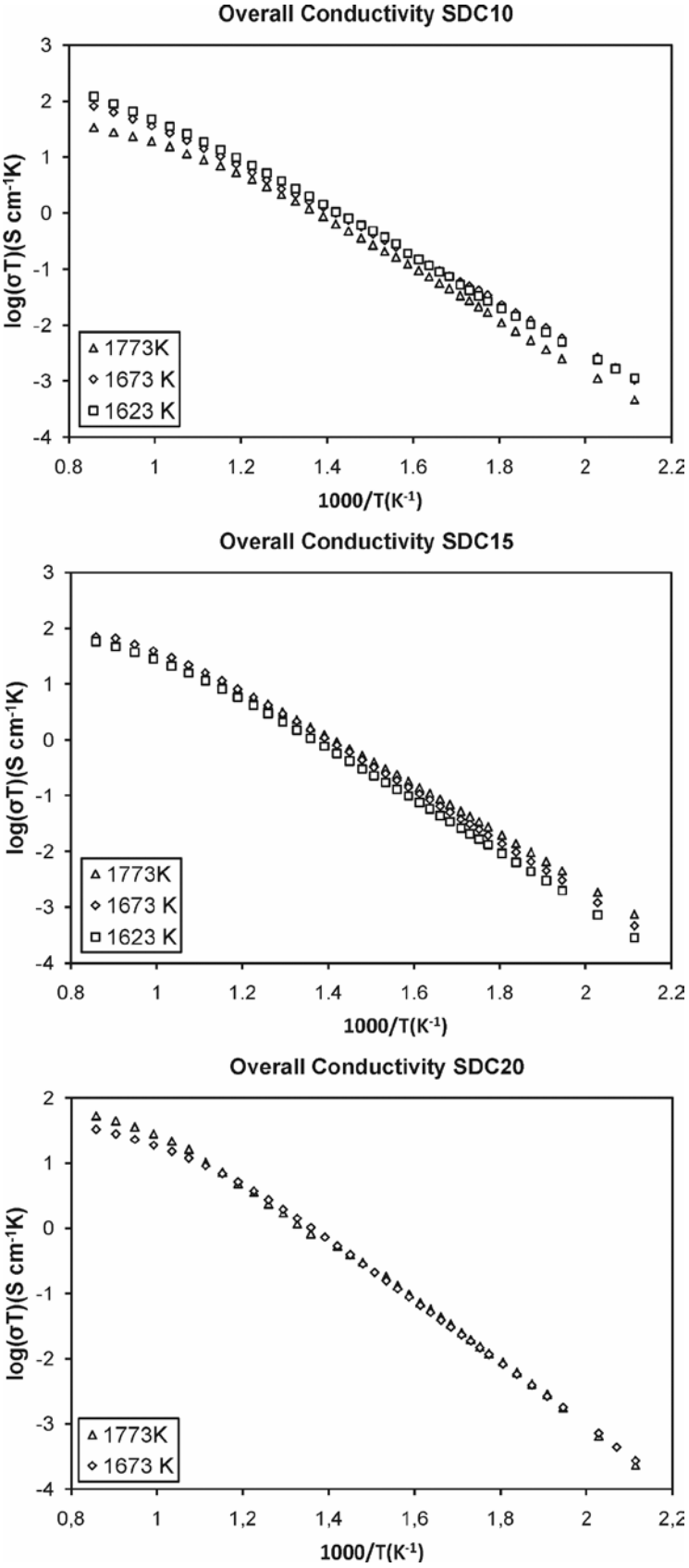

Figure 4. Overall Conductivity Arrhenius plots of SDC10 (up), SDC15 (middle) and SDC20 (bottom) samples

The typical evolution of the grain size for SDC10 samples with sintering temperature is depicted in Figure 2. Nearly fully dense pellets (≈99% density) are obtained, for the range of temperatures tested. However, a few intergranular remaining pores may be found in the pellets sintered at 1673 and 1623 K, lowering density values to around 95%. The observed microstructures are homogeneous and uniform along the specimens. The average grain sizes for all the specimens are given in Table I. A marked increase of almost one order of magnitude is observed between the samples with finer to those with coarser grain size.

3.2. Electrical conductivity

The analysis of the impedance spectra was carried out considering the brick-layer model (16). Conductivity values were obtained taking into account the sample geometry using the equation:

$$\sigma_i = \frac{L}{AR_i} \qquad [1]$$

where L is the sample thickness, A the electrode area, and R_i the overall, bulk or grain boundary resistance obtained by equivalent circuit analysis.

If a cubic grain shape and homogeneous grain boundary is assumed, it is possible to relate the measured electrical properties of the material: apparent grain boundary conductivity (σ_{gb}) and grain boundary capacitance (C_{gb}) to the electrical grain boundary thickness (δ_{gb}) and grain size (d_g) as follows:

$$C_{gb}\frac{L}{A} = \varepsilon_0 \varepsilon_{gb}\frac{d_g}{\delta_{gb}} \qquad [2]$$

where ε_0 and ε_{gb} are the vacuum and grain boundary permittivities respectively. Hence one may define the following relationship:

$$\frac{\delta_{gb}}{d_g} = \frac{C_b}{C_{gb}}\frac{\varepsilon_{gb}}{\varepsilon_b} \qquad [3]$$

where C_b stands for bulk capacitance. This permits to relate the measured apparent grain boundary with the specific grain boundary which is independent of the sample volume as:

$$\sigma^*_{gb} = \left(\frac{\delta_{gb}}{d_g}\right)\sigma_{gb} \qquad [4]$$

According to Guo *et al.* (6), it is appropriate to assume that the dielectric constant of the electrical grain boundary ε_{gb} approaches that of the bulk (ε_b) and then,

$$\frac{\delta_{gb}}{d_g} \approx \frac{C_b}{C_{gb}} \qquad [5]$$

Consequently, substituting this expression into eq. 4 a simple approximate equation for specific grain conductivity is obtained:

$$\sigma^{*}_{gb} = \left(\frac{C_b}{C_{gb}}\right)\sigma_{gb} \qquad [6]$$

One limitation of this method (14) is associated to a possible experimental error in the measurement of the bulk capacity. In order to limit this, bulk capacities have been calculated only in the low temperature regime (below 514 K) and when the bulk arc is completely defined.

From eq. 5 it is also possible to estimate the electrical grain boundary thickness, i. e. the length of the space charge layers. This value is usually reported to range between 1 and 5 nm depending on the nature of electrolyte (6). In this work, all the calculated grain boundary thicknesses are given in Table I and match the values given in literature.

Since electrical conduction in ceramics is thermally activated, these processes are suitable to be represented by fitting data to the Arrhenius equation:

$$\sigma T = \sigma_0 e^{\frac{-E_a}{kT}} \qquad [7]$$

where E_a is the activation energy for the conduction process, T the temperature, σ_0 the pre-exponential factor and k the Boltzmann constant. For all samples, the activation energy for the conduction process is estimated considering eq. 7 for the overall, bulk and grain boundary conduction processes. In the case of overall conductivity, the activation energy is calculated below 773 K.

The equivalent circuit analysis performed permits to separate and ascribe the two highest frequency semicircles of the complex impedance spectra to the bulk and grain boundary conduction processes. Each semicircle is simulated by a combination of a resistor and a constant phase element in parallel (*RQ*). The capacitance can be calculated using the following equation:

$$C = \frac{(RQ)^{1/n}}{R} \qquad [8]$$

All the calculated capacitances for the samples evaluated were in the typical range for bulk and grain boundary capacitances for ceria based electrolytes, i.e. $\approx 5\times10^{-11}$ F (bulk) and $\approx 10^{-8}$ F (grain boundary) respectively (17). Figure 3 shows the complex impedance plots normalised by geometric factor, measured at 473 K. As expected, the response corresponding to the bulk remains constant within a given composition and the overall response therefore depends mostly on the grain boundary contribution (Figure 4). The typical change in slope associated to the dissociation of defect complexes is observed for temperatures above 773 K in all cases. The highest value of overall conductivity at 773 K corresponds to the SDC10 sample sintered at lower temperature and hence with a finer grain size, i.e. 4.8×10^{-3} Scm^{-1}. However, the highest levels of conductivity vary with the composition and hence SDC15 exhibits the best performances when sintered at 1773 K (4.0×10^{-3} Scm^{-1}), whereas for SDC20 samples the overall conductivity is almost independent of the grain size, e.g. 2.5×10^{-3} Scm^{-1}. The explanation to this behavior is

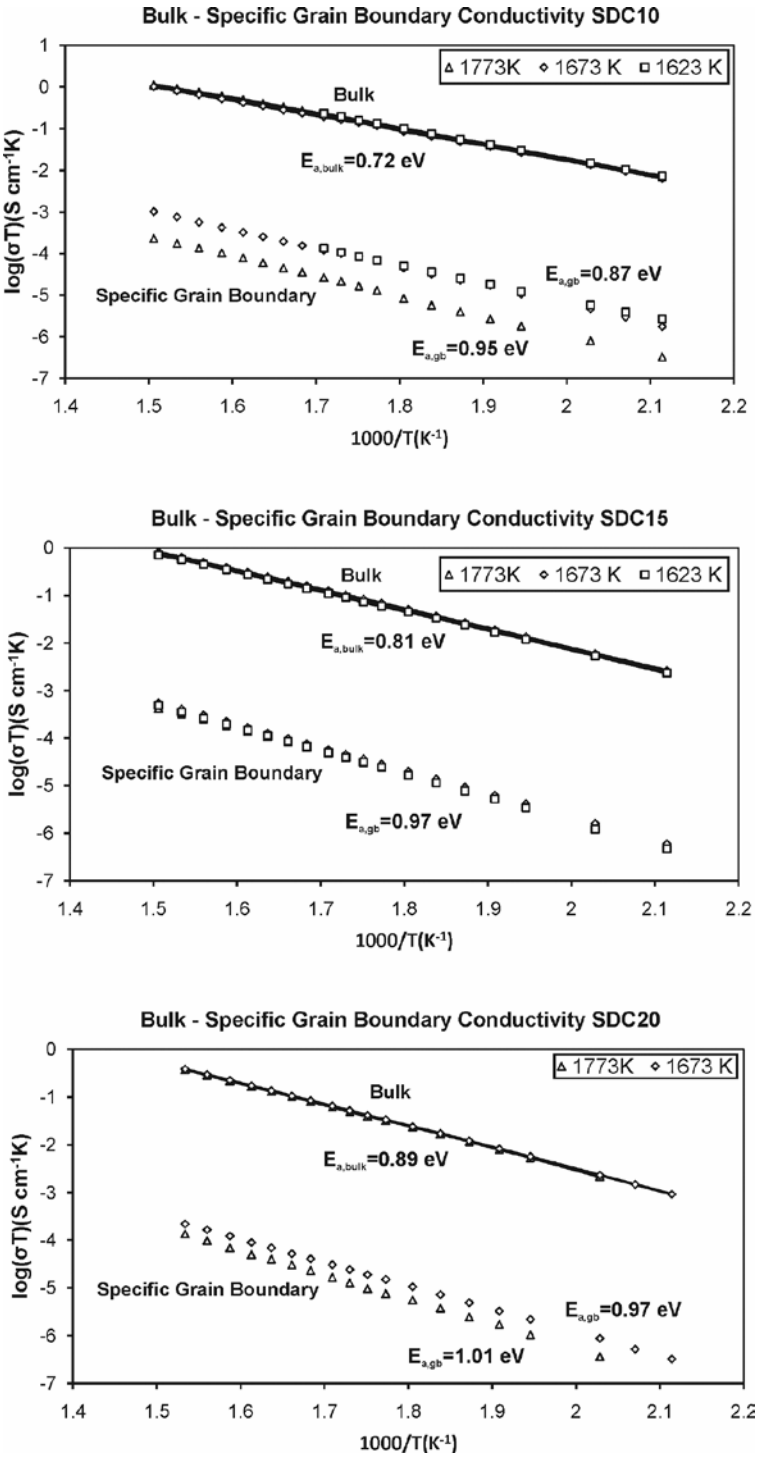

Figure 5. Bulk and specific grain boundary conductity Arrhenius plots of SDC10 (up), SDC15 (middle) and SDC20 (bottom) samples

not clear yet, although as the bulk conductivity remains independent of the grain size, this change is obviously associated to grain boundary electrical response, perhaps related to different levels of dopant segregation as a function of both the sintering temperature and migration enthalpies. Further analysis of published data (2,10) reveals that the lanthanide selected for doping may also have an important influence in the specific grain boundary conductivity and further investigations are highly demanded to determine their nature. Nevertheless and although the best results have been obtained for the lower dopant grade, all the conductivities are in the same order of magnitude and in agreement with the results obtained by Esposito *et al*. (17) for SDC20 sintered both conventionally and under a fast firing process or by Pérez-Coll *et al.* (18) obtained from freeze-dried precursors.

Figure 5 shows the low temperature Arrhenius plots of bulk and specific grain boundary conductivity. The activation energies for both conduction processes are also detailed. As mentioned above, one noticeable fact is that the bulk conductivity does not vary as a function of the grain size for any of the compositions evaluated in this range of sintering temperatures. Thus, no depletion of samarium in the grain interior is caused by the increase in the sintering temperature from 1623 to 1773 K. At temperatures below 773 K, activation energy for bulk conduction in SDC10 is 0.72 eV, and is linearly increased with the chemical composition up to 0.81 eV for SDC15 and 0.89 eV for SDC20. In this particular case, the increase in the activation energy of the bulk conductivity with the samarium content is accompanied by a decrease in the bulk conductivity itself. The highest bulk conductivity at 773 K was observed in SDC10 samples, with a value of 1.0×10^{-2} Scm^{-1}. This value decreases slightly to 7.9×10^{-3} Scm^{-1} and 6.0×10^{-3} Scm^{-1} for SDC15 and SDC20 respectively, which is related to the increase in migration enthalpy due to defects interactions when the dopant content is increased. On the other hand, the specific grain boundary conductivities vary dramatically depending on the sintering temperature for one fixed composition like, e.g. SDC10, with differences higher than one magnitude order. In this particular case, although the grain boundary volume is highly larger in finer grain size samples and is still highly resistive, the overall performance overcomes that of the samples sintered at higher temperatures. This increase in the specific grain boundary conductivity for 10% Gd doped ceria has been observed by Zhou *et al.* (8) for lower grain sizes (0.15 – 1.10 μm). Christie *et al*. (7) also observed a similar behavior for CGO20, though in a different range of grain sizes and for a lower extent. Moreover, Mori *et al*. (2) showed different V-shape overall conductivity curves whose minimum depend on grain size, dopant grade and rare earth type. If one also considers the significant effect of impurities on electrical behavior of grain boundaries described by Jasper *et al*. (19), the scatter of results may stand not only for composition and grain size but also for the preparation method. Our experimental observations for other rare-earth doped cerias (20) suggest that the grain boundary specific conductivity may vary more intensely for the dilute range, but when the dopant grade increases, the differences tend to vanish like in the SDC15 or SDC20 samples, where the overall response is almost independent on grain size. A plausible explanation for this observation is that a greater amount of dopant may help to reduce the effect of impurities on the grain boundary specific conductivity. In this sense, Guo *et al*. (4), based on previous research stated that the grain boundary blocking effect tends to be reduced when the dopant grade is greater than 15%. This effect has been also noticed in this work when evaluating the blocking effect of the electric charge carriers at the grain boundaries. The grain boundary blocking factor defined as $\alpha_{gb}=R_{gb}/(R_{bulk}+R_{gb})$ has been calculated at 473 K for all samples and given in Table I. The results are obviously closely related to the observed evolution of the specific grain boundary conductivities and exhibit a similar trend. For SDC10, α_{gb} increases with the sintering temperature, up to values of 0.93 for the largest grain sizes, whilst in SDC15 samples occurs the opposite and is independent of the grain size in SDC20. This suggests the existence of a complex relationship between sintering temperature, dopant concentration and optimal electrochemical properties.

4. CONCLUSIONS

Three compositions of samaria doped ceria (10, 15 and 20% at. samarium content) have been produced by the sol-gel method and sintered to almost full density with temperatures as low as 1623 K without the use of extremely high pressures, isostatic presses or sintering aids. The influence of the sintering temperature (hence grain size) on the overall and specific grain boundary conductivity has been evaluated, leading to the following conclusions:

In the range of grain sizes studied, the bulk conductivity is independent on the sintering temperature for the three compositions. This suggests the absence of a temperature promoted solute segregation to the grain boundary even at sintering temperatures as high as 1773 K.

The highest overall conductivity at 773 K is observed for SDC10 sintered at 1623 K. An increase in dopant content results in a decrease of the bulk conductivity.

The specific grain boundary conductivity depends strongly on the grain size for the lowest dopant grade, and this dependence is reduced when the samarium content increases. In the first case, differences greater than an order of magnitude have been observed.

The grain boundary blocking factors tend to decrease when the dopant content is increased, mostly due to the increase in bulk resistivity.

In other words, the preparation route and nature of the precursors largely affects the overall conductivity of ceria-based electrolytes. Therefore, a precise control over certain fabrication parameters such as the precursor particle size is crucial to produce electrolytes for IT-SOFCs exhibiting improved electrochemical responses.

ACKNOWLEDGEMENTS

The authors acknowledge financial support from Spanish Government (MAT-64486-07-C07, and "Ramón y Cajal" and "Juan de la Cierva" research fellowship programs), JCCM (PAC08-0183-9399), Universidad de Castilla-La Mancha and the Albacete Science & Technology Park.

REFERENCES

1. M. Mogensen, D. Lybye, K. Kammer, N. Bonanos, «Ceria Revisited: Electrolyte or Electrode Material» , pp. 1068-1074 en Solid Oxide Fuel Cells IX (SOFC IX), International symposium on solid oxide fuel cells 9, Quebec (Canada), Mayo 2005, Ed. J. Mizusaki, Subhash C. Singhal, The Electrochemical Society, New Jersey, (EE.UU.) 2005
2. T. Mori, R. Buchanan, D.R. Ou, F. Ye, T. Kobayashi, J.D. Kim, J. Zou, J. Drennan, «Design of nanostructured ceria-based solid electrolytes for development of IT-SOFC», J. Solid State Electrochem, 12, 841-849 (2008)
3. M.G. Bellino, D.G. Lamas, N.E. Walsöe de Reca. «Enhanced Ionic Conductivity in Nanostructured Heavily Doped Ceria Ceramics» Adv. Funct. Mater., 16, 107-113 (2006)
4. X. Guo, W. Sigle, J. Maier, «Blocking Grain Boundaries in Yttria-Doped and Undoped Ceria Ceramics of High Purity», J. Am. Ceramic. Soc., 86 [1], 77-87 (2003)
5. D. Pérez-Coll, P. Núñez, J.C. Ruiz-Morales, J. Peña-Martínez, J.R. Frade, «Re-examination of bulk and grain boundary conductivities of $Ce_{1-x}Gd_xO_{2-\square}$ ceramics», Electrochim. Acta, 52, 2001-2008 (2007)
6. X. Guo, R. Waser, «Electrical properties of the grain boundaries of oxygen ion conductors: acceptor-doped zirconia and ceria», Prog. Mater. Sci., 51, 151-210 (2006)
7. G.M. Christie, F.P.F van Berkel, «Microstructure-ionic conductivity relationships in ceria-gadolinia electrolytes», Solid State Ionics, 83, 17-27 (1996)
8. X.D. Zhou, W. Huebner, I. Kosacki, H.U. Anderson, «Microstructure and Grain-Boundary Effect on Electrical Properties of Gadolinium-Doped Ceria» J. Am. Ceramic. Soc., 85 [7], 1757-62 (2002)
9. Y. Wang, T. Mori, J.G. Li, J. Drennan, «Synthesis, characterization and electrical conduction of 10 mol% Dy_2O_3-doped CeO_2 ceramics» J. Eur. Ceram. Soc., 25, 949-956 (2005)
10. D.R. Ou, T. Mori, F. Ye, M. Takahashi, J. Zou, J. Drennan, «Microstructure and electrolytic properties of yttrium-doped ceria electrolytes: Doped concentration and grain size dependences» Acta Mater., 54, 3737-3746 (2006)
11. Johnson D. ZView: A software Program for IES Analysis,Version 2.9c, Scribner Associates, Inc., 2005.
12. A.J. Dos santos-García, C. Sánchez-Bautista, J. Canales-Vázquez, Precursor Particle Size vs. Ionic Radii in Rare Earth Doped Ceria: A Remarkable Gaussian Correlation, to be published.
13. W. Huang, P. Shuk, M. Greenblatt «Properties of sol-gel prepared $Ce_{1-x}Sm_xO_{2-x/2}$ solid electrolytes» Solid State Ionics, 100, 23-27 (1997)
14. D.D. Upaddhyaya, R. Bhat, S. Ramanathan, S.K. Roy, H. Schubert, G. Petzow, «Solute Effect on Grain Growth in Ceria Ceramics» J. Eur. Ceram. Soc., 14, 337-341 (1994)
15. J. Fleig, J. Maier, «The Impedance of Ceramics with Highly Resistive Grain Boundaries: Validity and Limits of the Brick Layer Model» J. Eur. Ceram. Soc., 19, 693-696 (1999)
16. M.J. Verkerk, B.J. Middelhuis, A.J. Burggraaf, «Effect of Grain Boundaries on the Conductivity of High-Purity ZrO_2-Y_2O_3 Ceramics» Solid State Ionics, 6, 159-170 (1982)
17. V. Esposito, E. Traversa, «Design of Electroceramics for Solid Oxides Fuel Cells Applications: Playing with Ceria», J. Am. Ceram. Soc., 91 [4], 1037-1051 (2008)
18. D. Pérez-Coll, P. Núñez, J.R. Frade, J.C.C. Abrantes, «Conductivity of CGO and CSO ceramics obtained from freeze-dried precursors», Electrochim. Acta, 48, 1551-1557 (2003)
19. A. Jasper, J.A. Kilner, D.W. McComb, «TEM and impedance spectroscopy of doped ceria electrolytes» Solid State Ionics, 179, 904-908 (2008)
20. C. Sánchez-Bautista, A. Dos santos-García, J. Peña-Martínez, J. Canales-Vázquez, «The grain boundary effect on dysprosium doped ceria», to be published.

Recibido: 30-6-09
Aceptado: 30-11-09